A Spatial Model of Wind Shear and Turbulence

C Warren Campbell*
NASA Marshall Space Flight Center, Huntsville, Alabama
and
V A Sanborn†
Colorado State University, Fort Collins, Colorado

Recently, the Joint Airport Weather Studies (JAWS) Project Office released wind shear data sets measured with Doppler radar. The JAWS microburst data are the best wind shear measurements ever made, but do not contain all turbulence response frequencies of a landing aircraft. A typical JAWS grid spacing is 200 m, while a desired spacing is on the order of 10 m The spatial model reported herein adds three dimensional Monte Carlo simulated turbulence to the JAWS data The three dimensional added turbulence is based on the von Kármán spectra, is isotropic, and contains variation in all three coordinate directions The JAWS data cover a volume typically 12×12×1.5 km. Because of the higher sampling rate the generated turbulence cannot fill the entire JAWS volume and still represent a manageable data base The JAWS volume is filled by generating a manageable block of turbulence and in effect stacking the blocks By generating the turbulence non dimensionally, the turbulence length scale can vary throughout the JAWS volume In a flight simulation, the spatial model permits the calculation of all aerodynamic loads and moments by simulation of the spatial variation of winds over the body of an aircraft

Nomenclature

$H_i(\nu_1)$	= one-dimensional transfer function for ith velocity component
$H_i(\nu_1\ \nu_2\ \nu_3)$	= three-dimensional transfer function for ith velocity component
k_i	= ith index in transform (FFT) domain
L	= length scale of turbulence
n_i	= ith index in space domain
u_i	= simulated ith component of wind
$\bar{u}_i$	= ith velocity component interpolated from JAWS data
w_i	= ith component of simulated wind
$x(n_1)$	= one dimensional digital function
$x(n_1,n_2)$	= two-dimensional digital function
$x(n_1\ n_2\ n_3)$	= three dimensional digital function
$X(k_1)$	= FFT of $x(n_1)$
$X(k_1\ k_2)$	= FFT of $x(n_1,n_2)$
$X(k_1\ k_2\ k_3)$	= FFT of $x(n_1\ n_2\ n_3)$
δ_{ij}	= Kronecker delta
$\theta_{ij}(\nu_1)$	= one-dimensional spectrum $\int_{-\infty}^{\infty}\int \Phi_{ij}(\nu_1\ \nu_2\ \nu_3)\mathrm{d}\nu_2\mathrm{d}\nu_3$
ν_i	= ith spatial frequency
σ_i	= ith component gust standard deviation
$\Phi_{ij}(\nu_1\ \nu_2\ \nu_3)$	= three dimensional spectrum function

Introduction

GEOMETRIC characteristics of some of the recently acquired JAWS multiple Doppler data sets are summarized in Table 1 A typical grid spacing is 200 m With this grid spacing, turbulence with length scales shorter than 400 m are not contained in the JAWS data For a landing speed of 80 m/s the JAWS data is truncated at 0 2 Hz The JAWS data contains only part of the short-period aircraft response frequencies and fewer of the aircraft structural frequencies Figure 1 shows dimensionless one dimensional spectral functions θ_{11} and θ_{22} multiplied by frequency and plotted as a function of logarithmic frequency E is the Heisenberg spectral function The form of the plots i e., $f\phi_{ii}$ vs ℓnf is area-preserving. Hence, the energies at frequencies higher than the JAWS cutoff is proportional to the areas under the curves to the right of the cutoff The three plots are at different turbulent length scales, i e , $L = 500$, 1000 and 1500 m These are typical of length scales measured by NASA's Gust Gradient aircraft although some length scales were shorter than 200 m From Fig 1 a significant portion of the higher frequency energy is truncated from the JAWS data Aircraft frequency response extends well beyond the JAWS cutoff The aircraft structural frequencies are sometimes neglected in flight simulations and may be the source of pilot complaints concerning the incorrect "feel" of simulated turbulence A passenger in an aircraft feels acceleration of the aircraft center of gravity and the ringing response of the airframe [1] Some simulators include airframe structural response modes for this reason.

The implication of Fig 1 and of the above discussion is that turbulence must be added to the JAWS wind shear data base The approach taken in this study was to add Monte Carlo simulated turbulence as realistically as possible Providing gust environment inputs so that all aerodynamic loads and moments can be calculated requires knowledge of the variation of wind over the aircraft body Etkin[2] has suggested that gust gradients be simulated along with gusts, and Tatom et al.[3] have implemented this suggestion In actual fact, gusts cannot be considered linear across an airfoil as has been shown by NASA's B 57B Gust Gradient Program. Other objections to the simulation of gust gradients, as proposed by Tatom et al ,[3] are discussed by Campbell [4] For the reasons described above and in the references, a three dimensional approach to turbulence simulation was taken For the purposes of this paper, one dimensional turbulence simulation refers to simulation of variation of the three velocity components along the flight path only Lateral and vertical

Presented as Paper 84 0277 at the AIAA 22nd Aerospace Sciences Meeting Reno, Nev Jan 9 12 1984; received Feb 2 1984; revision received May 23 1984 This paper is declared a work of the U S Government and therefore is in the public domain

*Aerospace Engineer Atmospheric Sciences Division Systems Dynamics Laboratory

†Professor Department of Civil Engineering Member AIAA

correlations of turbulent gusts are neglected in one dimensional simulations. This paper presents a fully three dimensional simulation, i e , variation of each velocity component over all three space dimensions

Overview of the Spatial Model

In the preceding section, the need for adding turbulence to the JAWS data was described The means of adding the turbulence is described in this section The "glue" which holds the spatial model together is the following equation:

$$u_i(x\ y\ z\ t) = \bar{u}_i(x\ y\ z\ t) + \sigma_i(x\ y\ z,t)\ w_i(x\ y\ z) \qquad (1)$$

where $u_i(x\ y\ z\ t)$ are the simulated wind components; $\bar{u}_i(x\ y\ z\ t)$ the low frequency wind components provided in the JAWS first moment (velocity) data; and $\sigma_i(x\ y,z,t)$ the components of gust intensity associated with the high-frequency turbulence Estimates of σ_i can be obtained from JAWS second moment (spectral width) data $w_i(x,y,z)$ are the three components of Monte Carlo simulated turbulence The model of Eq (1) is similar to a one dimensional model proposed by Mark[5] for data analysis

In Eq. (1) a variation in time is indicated for the simulated wind u_i, and in the JAWS information. In fact, the JAWS project office has chosen not to expend the resources required for creating a time-varying data base The spatial model is general enough to handle transient phenomena and the equation was written is the more general form

In Eq (1), w_i represents a "frozen" turbulence data base created by Monte Carlo simulation A three-dimensional block for each component can be generated Generation of the block of frozen turbulence was done a priori One dimensional turbulence is often generated in real time using methods based on z transform theory In these cases generation of the turbulence is achieved quickly with a relatively simple recursion relation z transform theory is not well developed in two or more dimensions Generation of the three-dimensional turbulence cannot be done using z trans forms because the three dimensional spectral functions are nonseparable The block of turbulence, therefore, must be generated ahead of time

The three-dimensional spectral functions for isotropic turbulence are written in terms of a constant length scale, L L varies through space in the real atmosphere Microbursts interact with the planetary boundary layer (PBL) in such a way as to affect the spatial distribution of the turbulent length scale From these facts, the frozen turbulence must be generated in such a way that the length scale can vary in an arbitrary fashion. This goal was achieved by generating the turbulence nondimensionally In dimensionless space the block has a constant "volume " In dimensional space the size of the block changes with the length scale With increasing length scale the block grows larger Conversely in the dimensional frequency domain, the spectral block decreases with increasing length scale For flight simulation the dimensionless turbulence is converted to dimensional tur bulence

Only a limited volume of turbulence can be generated because of the much higher sampling frequency of turbulence as compared with the JAWS grid spacing Filling the JAWS volume with turbulence was achieved by effectively stacking the single block throughout the JAWS volume Two ways of stacking the turbulence were considered One way is to stack copies of the same block in the same orientation to fill the total simulation volume This method could conceivably cause discontinuities in the turbulence as the simulated flight proceeds out one side of the block and enters the opposite face An alternative approach is to reflect the aircraft velocity at each face of the block This procedure avoids any discontinuity in the turbulence. The flight can be pictured in

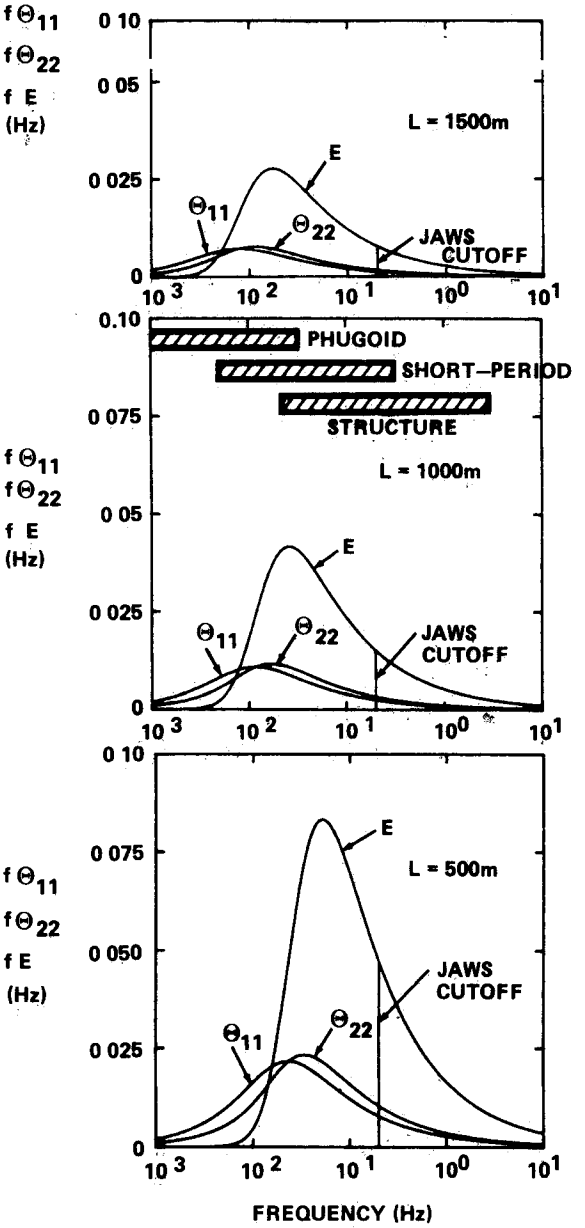

Fig 1 Spectral truncation in the JAWS data sets

Table 1 JAWS dual Doppler cases

Date	Δx[a] m	Δy[b] m	Δz[c] m	RV_{max} m/s	No of $x \times y \times z$ grid points
June 29, 1982	300	300	250	25	$60 \times 60 \times 9$
July 14 1982	200	200	150	30	$60 \times 60 \times 11$
August 5 1982	150	150	250	30	$81 \times 81 \times 9$

[a] Δx is the east west grid spacing. [b] Δy is the north south grid spacing [c] Δz is the vertical grid spacing

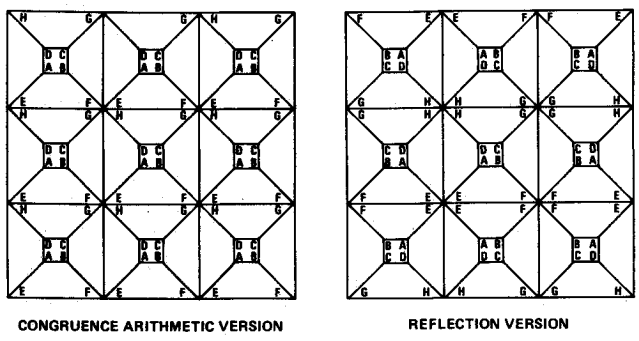

Fig 2 Stacking strategies for blocks of frozen turbulence

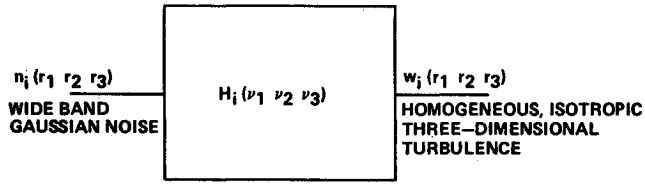

Fig 3 Generation of three-dimensional turbulence

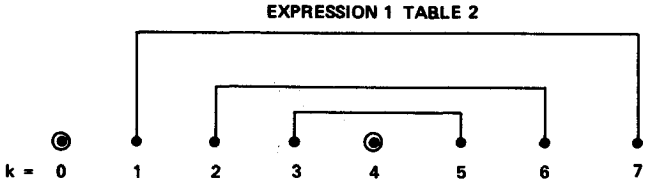

Fig 4 Correspondence of complex conjugate pairs in the one-dimensional transform domain

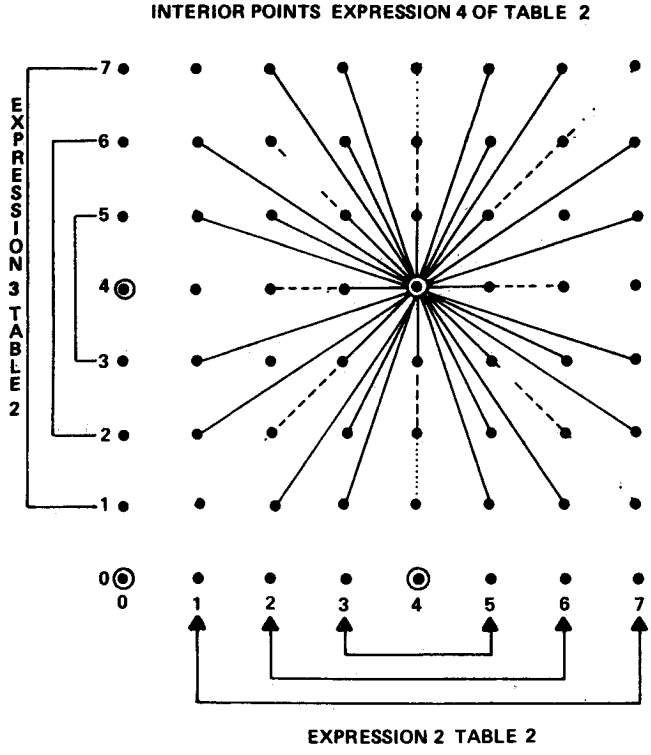

Fig 5 Correspondence of complex conjugate pairs in the two dimensional transform domain.

the two dimensional case by consideration of a video game with a "ball" moving on the screen In the first case, as the ball leaves the screen on one side it reappears instantaneously on the other side In the second example as the ball ap proaches the edge of the screen it bounces off the edge and passes back across the screen The effective stacking strategies for the two procedures are depicted in Fig 2 Each of the nine large squares at the top and bottom of the figure is topologically identical to a rectangular solid Each of the eight corners is labeled with a letter The top half of the figure depicts nine identical blocks stacked in the same orientation The bottom figure depicts nine blocks also Inspection reveals that the bottom stack consists of two different types of blocks (reflections of each other) stacked in different orientations to avoid any possible discontinuities

The first method can be implemented using congruence arithmetic as follows:

$$x_T = x \bmod (x_{T\max})$$

$$y_T = y \bmod (y_{T\max})$$

$$z_T = z \bmod (z_{T\max}) \qquad (2)$$

In this equation $(x\ y\ z)$ represents the location of the plane in space $(x_T\ y_T\ z_T)$ the plane location within the block of turbulence and $(x_{T\max}, y_{T\max}\ z_{T\max})$ the maximum dimensions of the block of frozen turbulence The notation of Eq (2) means take x divide by $x_{T\max}$, and take the remainder which is x_T Do the same for y_T and z_T From the equation $0 \le x_T \le x_{T\max}$, $0 \le y_T \le y_{T\max}$, and $0 \le z_T \le z_{T\max}$ The congru ence method has the advantage of computational simplicity over the reflection method and in practice the expected discontinuities did not materialize Hence, the congruence method was used for turbulence block stacking

Contraction and expansion of the block of turbulence with changing length scale were discussed earlier When the blocks are stacked, changing length scale causes the whole stack to change size If the center of contraction is some distance from the simulated aircraft then turbulence will be moved past the plane not as a result of the plane's motion but rather because of the contraction This dilemma was avoided by making the center of contraction at the airplane

The JAWS data and the frozen turbulence are defined on a discrete grid. To define winds between grid points some method of interpolation must be selected JAWS data in terpolation is described in a later section Some guidance concerning turbulence interpolation is given by Tatom and Smith [6] who recommend zeroth order (stair step) interpo lation. This is the approach used herein

Frozen Turbulence Generation

Three dimensional frozen turbulence is generated using Monte Carlo methods as shown in Fig 3 Gaussian, three dimensional, white noise is input to a linear, three dimensional filter A Gaussian process input to a linear filter results in a Gaussian output process The transfer function was selected to give the desired output spectrum

More than one implementation of Fig 3 is conceivable The most obvious approach is to generate the noise in the space domain, transform to the frequency domain, multiply point by point by the transfer function and then transform back to the space domain This approach requires two Fourier transforms and even with fast Fourier transforms (FFT) the procedure is time consuming An alternative is to generate the noise in the frequency domain, multiply by the transfer function, and transform back to the space domain In this way one of the Fourier transforms is eliminated A discussion of frequency domain noise generation is given in Ref 7

Generation of turbulence in the frequency domain is done using the results of Tables 2 and 3 Table 2 gives values of the

Table 2 Symmetry properties of transformed one , two , and three dimensional digital functions

Expression	Observation
One dimensional symmetry	
1) $X(M-k)=X^*(k)$	$\mathrm{Im}[X(M/2)]=0$
Two dimensional symmetry	
2) $X(M_1-k_1\ 0)=X^*(k_1\ 0)$	$\mathrm{Im}[X(M_1/2,0)=0]$
3) $X(0\ M_2-k_2)=X^*(0\ k_2)$	$\mathrm{Im}[X(0\ M_2/2)=0]$
4) $X(N_1-k_1\ N_2-k_2)=X^*(k_1\ k_2)$	$\mathrm{Im}[X(M_1/2\ M_2/2)=0]$
Three dimensional symmetry	
5) $X(M_1-k_1\ 0\ 0)=X^*(k_1\ 0\ 0)$	$\mathrm{Im}[X(M_1/2\ 0\ 0)]=0$
6) $X(0\ M_2-k_2\ 0)=X^*(0\ k_2\ 0)$	$\mathrm{Im}[X(0\ M_2/2\ 0)]=0$
7) $X(0\ 0\ M_3-k_3)=X^*(0,0,k_3)$	$\mathrm{Im}[X(0\ 0\ M_3/2)]=0$
8) $X(M_1-k_1\ M_2-k_2,0)=X^*(k_1\ k_2\ 0)$	$\mathrm{Im}[X(M_1/2\ M_2/2\ 0)]=0$
9) $X(M_1-k_1\ 0\ M_3-k_3)=X^*(k_1\ 0\ k_3)$	$\mathrm{Im}[X(M_1/2\ 0\ M_3/2)]=0$
10) $X(0\ M_2-k_2\ M_3-k_3)=X^*(0\ k_2\ k_3)$	$\mathrm{Im}[X(0,M_2/2\ M_3/2)]=0$
11) $X(M_1-k_1\ M_2-k_2\ M_3-k_3)=X^*(k_1\ k_2\ k_3)$	$\mathrm{Im}[X(M_1/2\ M_2/2\ M_3/2)]=0$

Table 3 Expected value and variance of transformed one and three dimensional noise with zero mean value

One dimensional case

$$X_k=\sum_{n=0}^{M-1} x_n \exp(-j2\pi nk/M)\,\Delta r$$

1) $E[X_k]=0$

2) $\sigma_{x_k}^2=E[X_kX_k^*]=M(\Delta r)^2\sigma_{x_n}^2$

3) $E[X_lX_l^*]=M(\Delta r)^2\sigma_{x_n}^2\delta kl$

4) $E[\mathrm{Re}^2(X_k)]=M(\Delta r)^2\sigma_{x_n}^2[1/2+1/2\,\delta 0k+1/2\,\delta_{M/2k}]$

5) $E[\mathrm{Im}^2(X_k)]=\dfrac{M(\Delta r)^2\sigma_{x_n}^2}{2}[1-\delta 0k-\delta_{M/2\,k}]$

6) $E[\mathrm{Re}[X_k]\,\mathrm{Im}[X_l]]=0$ for all l and k

Three dimensional case

$$X_{k_1\ k_2\ k_3}=\sum_{n_1=0}^{M_1-1}\sum_{n_2=0}^{M_2-1}\sum_{n_3=0}^{M_3-1} x_{n_1\ n_2\ n_3}\exp[-j2\pi(n_1k_1/M_1+n_2k_2/M_2+n_3k_3/M_3)]\Delta r_1\Delta r_2\Delta r_3$$

7) $E[X_{k_1\ k_2\ k_3}]=0$

8) $\sigma_{xk}^2=E[X_{k_1\ k_2\ k_3}X^*{}_{k_1\ k_2\ k_3}]=M_1M_2M_3\sigma_{xn}^2(\Delta r_1\Delta r_2\Delta r_3)^2=M_1M_2M_3\sigma_{xn}^2/(\nu_{s_1}\nu_{s_2}\nu_{s_3})^2$

9) $E[X_{k_1\ k_2\ k_3}X^*{}_{l_1\ l_2\ l_3}]=[M_1M_2M_3\sigma_{xn}^2/(\nu_{s_1}\nu_{s_2}\nu_{s_3})^2]\delta_{k_1l_1}\delta_{k_2l_2}\delta_{k_3l_3}$

10) $E[\mathrm{Re}^2(X_{k_1\,k_2\,k_3})]=\dfrac{M_1M_2M_3\sigma_{xn}^2}{2(\nu_{s_1}\nu_{s_2}\nu_{s_3})^2}[1+(\delta_{0k_1}+M_1/2\ k_1)(\delta_{0k_2}M_2/2\,k_2)(\delta_{0k_3}+\delta M_3/3\,k_3)]$

11) $E[\mathrm{Im}^2(X_{k_1\ k_2\ k_3})]=\dfrac{M_1M_2M_3\sigma_{xn}^2}{2(\nu_{s_1}\nu_{s_2}\nu_{s_3})^2}[1+(\delta_{0k_1}+\delta M_1/2k_1)(\delta_{0k_2}+\delta M_2/2\,k_2)(\delta_{0k_3}+\delta M_3/2\,k_3)]$

12) $E[\mathrm{Re}(X_{k_1\ k_2\ k_3})\,\mathrm{Im}(X_{l_1\ l_2\ l_3})]=0$ for all $k_1\ k_2\ k_3, l_1\ l_2\ l_3$

variance and mean value of transformed noise Since the noise in the space domain is Gaussian, the transformed noise is also Gaussian In order for the space domain turbulence to have real values only certain Hermitian symmetries must be ob served These properties are summarized in Table 3 The one , two , and three dimensional symmetries of the transforms of real functions are presented in this table because each plays a part in the three dimensional Fourier transform Each of these symmetries is part of a simple guiding principle, i e , reflection about the center point Figures 4 and 5 show corresponding points for the one and two dimensional cases The same principle is true for the three dimensional case also Circled points in Figs 4 6 are points that reflect into them selves and, therefore must have real transform values

Table 3 contains the mean and standard deviations of transformed noise Since the noise is Gaussian and the FFT is a linear operation the transformed noise is also Gaussian Since the mean and variance are known, the transformed noise can be generated directly in the frequency domain

The three-dimensional von Kármán spectrum function Φ_{ii} is given in nondimensional form by

$$\Phi_{ii}(\nu_1\ \nu_2\ \nu_3) = \frac{440\pi^3}{9}\ \frac{a^4(\nu^2-\nu_i^2)}{[1+(2\pi a\nu)^2]^{17/6}} \tag{3}$$

where $a=1\ 339$, ν_i is the ith component of spatial frequency, and $\nu=(\nu_1^2+\nu_2^2+\nu_3^2)^{1/2}$. Φ_{33} is typical of Φ_{ii} If Φ_{33} is fixed, then ν_3 can be solved for

$$\nu_3 = \pm\sqrt{\left(\frac{C_1\rho^2}{\Phi_{33}}\right)^{6/17} - 1}\left]\frac{1}{C_2} - \rho^2\right. \tag{4}$$

where $\rho^2=\nu_1^2+\nu_2^2$ and C_1 and C_2 are constants

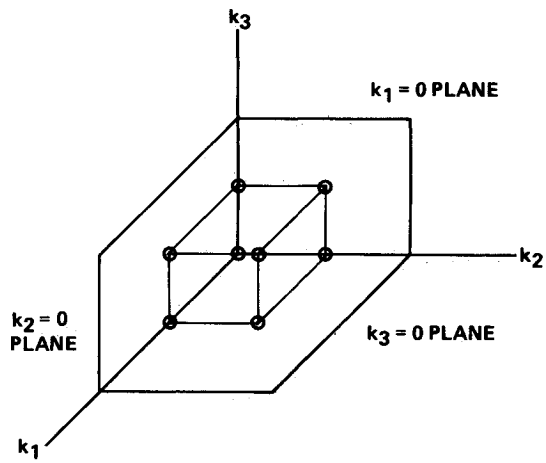

Fig 6 Points in the transform domain when the transform must be real

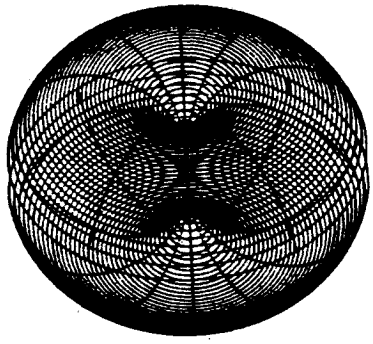

Fig 7 Perspective of surface of constant Φ_{33} for the von Kármán model

Equation (4) defines a surface of constant Φ_{33} and has rotational symmetry about the ν_3 axis A perspective view of the toroidal surface of constant Φ_{33} is given in Fig 7

Since the noise spectra are uniform only out to the sampling frequencies divided by two (Nyquist frequencies), a nor malization factor must be added to the transfer function Of the infinity of transfer functions possible, the zero phase transfer function was selected for this study

$$H_i(\nu_1\ \nu_2\ \nu_3) = \sqrt{\nu_{s_1}\nu_{s_2}\nu_{s_3}}\,\overline{\Phi_{ii}(\nu_1\ \nu_2\ \nu_3)}/\sigma_n \tag{5}$$

where $\nu_{s1}\ \nu_{s2}\ \nu_{s3}$ are the three sampling frequencies and σ_n is the noise standard deviation

Use of Wind Shear Data Sets with Simulated Turbulence

Interpolation of the JAWS data was accomplished using Langrange polynomial basis functions

$$\bar{u}(x\ y\ z) = \sum_{n=1}^{8} \bar{U}_n P_n(x,y\ z) \tag{6}$$

where $\bar{u}(x\ y\ z)$ is the interpolated quantity, $\bar{U}_n$ the value of the quantity at the surrounding eight grid points, and $P_n(x\ y\ z)$ the basis function associated with the nth grid point

Figure 8 shows a single cell in the interpolation grid Based on the axis arrangement shown in the figure, the basis functions are given in Table 4

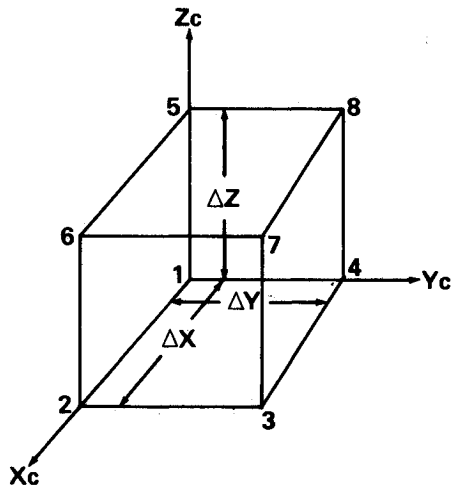

Fig. 8 Definition of interpolation variables

Table 4 Lagrange polynomial basis functions

$$P_1(x_c\ y_c\ z_c) = (\Delta x - x_c)(\Delta y - y_c)(\Delta z - z_c)/(\Delta x\,\Delta y\,\Delta z)$$

$$P_2(x_c\ y_x\ z_c) = x_c(\Delta y - y_c)(\Delta z - z_c)/(\Delta x\,\Delta y\,\Delta z)$$

$$P_3(x_c\ y_c\ \dot{z}_c) = x_c y_c(\Delta z - z_c)/(\Delta x\,\Delta y\,\Delta z)$$

$$P_4(x_c\ y_c\ z_c) = (\Delta x - x_c)\ y_c\ (\Delta z - z_c)/(\Delta x\,\Delta y\,\Delta z)$$

$$P_5(x_c\ y_c, z_c) = (\Delta x - x_c)(\Delta y - y_c)\ z_c/\Delta x\,\Delta y\,\Delta z\,\Delta z)$$

$$P_6(x_c\ y_c\ z_c) = x_c(\Delta y - y_c)\ z_c/(\Delta x\,\Delta y\,\Delta z)$$

$$P_7(x_c\ y_c\ z_c) = x_c y_c z_c/(\Delta x\,\Delta y\,\Delta z)$$

$$P_8(x_c\ y_c\ z_c) = (\Delta x - x_c)\ y_c\ z_c/(\Delta x\,\Delta y\,\Delta z)$$

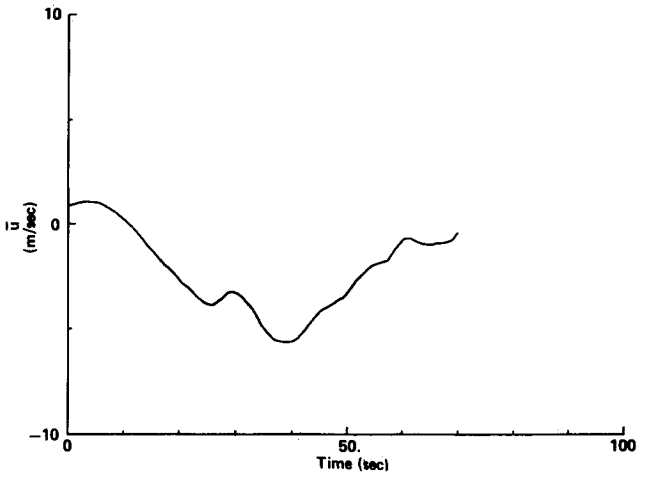

Fig 9 East west JAWS velocity on a simulated ILS approach (3 deg glide slope)

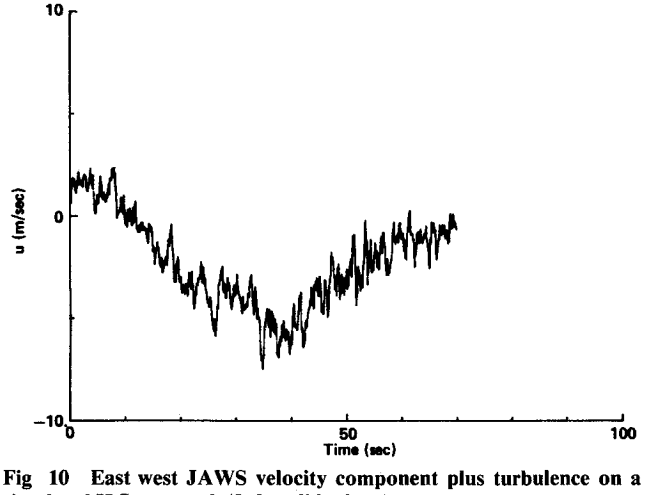

Fig 10 East west JAWS velocity component plus turbulence on a simulated ILS approach (3 deg glide slope)

To demonstrate the spatial model, a $64 \times 64 \times 64$ block of turbulence corresponding to the u velocity component was generated and added to the July 14 JAWS case as indicated in Eq (1) As of this writing, JAWS second moment data was unavailable and the distribution of gust intensity σ, had to be specified Based on logic described by Campbell[7] the following form of σ was used:

$$\sigma = \{\sigma_{\max} - (\sigma_{\max}/2) \exp[-(r/0\ 75)^2]\} \times \exp(-r^2/50) \exp[(z-300)/200] \quad (7)$$

where r is the horizontal distance from the microburst center at the surface (in kilometers) and Z is the altitude (in meters)

A simple relation for the length scale of turbulence was selected from Ref 8

$$L = 31\ 5\ (z/18\ 3)^{0\ 64}\ \text{m} \quad (8)$$

To demonstrate the model, a point airplane was passed through JAWS data and turbulence at a constant velocity The computer program permitted the selection of horizontal flight at any altitude or an ILS approach or departure (3 deg glide slope) Any of the three modes permitted the selection of a constant but arbitrary heading In addition, the program contained two "knobs": one of the knobs controlled wind shear and permitted it to be turned on or off the other permitted the turbulence to be turned up down, or off With

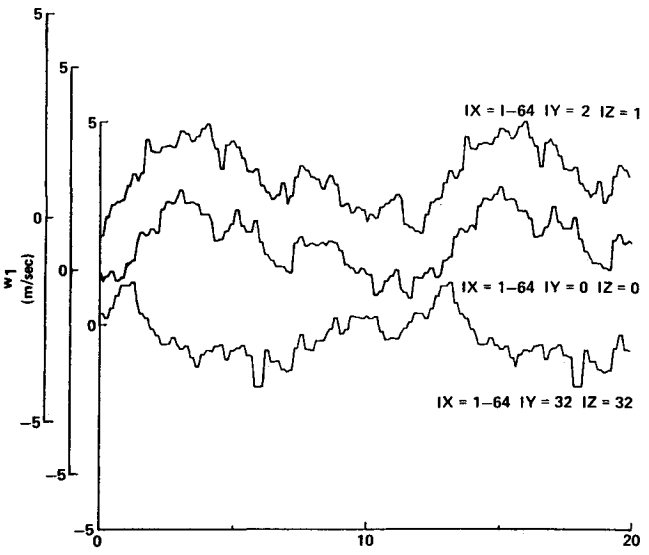

Fig 11 Comparison of lines of turbulence from the simulated turbulence

these knobs the wind shear could be examined without turbulence with turbulence, or the turbulence could be examined without wind shear Figure 9 shows the east west velocity component during an ILS approach through the July 14 JAWS case Figure 10 depicts the same run with turbulence added Energy in the higher frequencies increases toward the end of the run as the length scale decreases toward the ground

Figure 11 depicts horizontal passes through the block of turbulence The sampling rate was selected so that each grid point was contained in the traces The top two traces are adjacent lines of grid points in the frozen turbulence As expected these two curves show a high degree of correlation The top two curves are from an edge of the block The bottom curve is from a line parallel to the other two, but is taken from the center of the block The correlation between this curve and the other two is greatly reduced These three curves show the lateral and vertical falloff of the correlation for the turbulence model

Summary and Conclusion

The purpose of the spatial model is to generate the wind environment for use by others for flight simulation Winds and gusts are provided over any finite area (e g , aircraft body) from which aircraft loads and moments may be calculated Three dimensional autospectral information and correlation (Φ_{ii} and R_{ii}) are contained in these data The model does not contain cross spectral information, e g Φ_{12}, and it is not clear how to add this to the present model Nevertheless, this three dimensionality as contained in the spatial model affords much greater realism than widely used one dimensional models

The resulting simulated wind is a nonlinear non Gaussian combination of real atmospheric winds and Gaussian three dimensional turbulence modulated by gust intensities which may vary freely as desired over space The turbulence as represented by a product of a varying gust intensity and simulated turbulence is nonlinear and non Gaussian

Because of the three dimensionality of the spatial model results of a simulation are in no way degraded by performance of any maneuver This is in contradistinction to one dimensional simulations, especially where the radius of the turn is small compared to turbulent length scales

The spatial model is used primarily for in flight simulations of a general nature Gust intensity and length scale distributions must be provided by the user Generation of three dimensional turbulence is time consuming (~20 h for each component on Hewlett Packard F Series computers).

There are an infinite number of paths through the turbulence, but each path has some finite correlation with any other path because of the three dimensionality As a result, any attempt at flying numerous passes through the turbulence for the purposes of ensemble averaging is, strictly speaking, invalid

The spatial model could be used for real time simulations if sufficient memory were available to store the data The storage requirement is roughly the same as the JAWS velocity storage requirements for a typical case Obtaining values of turbulence would require access to three values, one for each velocity component

References

[1]Terry, C , Personal communication United Airlines Denver Colo Sept 1983.

[2]Etkin, B , *Dynamics of Atmospheric Flight* John Wiley and Sons Inc N Y 1972

[3]Tatom F B , Smith, S R , Fichtl G H and Campbell C W , Simulation of Atmospheric Turbulent Gusts and Gust Gradients ' *Journal of Aircraft* Vol 19 April 1982 pp 264 271

[4]Campbell W ' A Conceptual Framework for Using Doppler Radar Acquired Atmospheric Data for Flight Simulation NASA TP 2192 June 1983

[5]Mark, W D , ' Characterization Parameter Estimation and Aircraft Response Statistics of Atmospheric Turbulence NASA CR 3463 Sept 1981

[6]Tatom F B and Smith S. R 'Advanced Space Shuttle Simulation Model ' NASA CR 3541 April 1982

[7]Campbell W A Spatial Model of Wind Shear and Turbulence for Flight Simulation Ph D Dissertation, Colorado State University Fort Collins Colo ; to be published June 1984

[8]Kaufman, J W ed , 'Terrestrial Environment (Climatic) Criteria Guidelines for Use in Aerospace Vehicle Development 1977 Revision NASA TM 78118 Nov 1977